Powder Metallurgy & Mining

Micro Structural Evolution of a 93 Wt% Tungsten Heavy Alloy: A Quenching Study to Understand the Evolution of Contiguity, Connectivity with Sintering Temperature and Time

Bollina R*, Suri P, Park SJ and German RM

Associate Professor, School of Engineering and Technology, Mahindra Ecole Centrale, Bahadurpally, Jeedimetla, Hyderabad, Andhra Pradesh, India

Abstract

Sintering temperature and time have an effect on the densification and distortion of liquid phase sintered tungsten heavy alloys. Quenching was used to observe the *in situ* microstructure at different temperatures and times. A 93 wt.% tungsten heavy alloy (WNi-Fe) was quenched from different temperatures and from 1500°C at different hold times and the micro structural parameters such as contiguity, connectivity, and grain size which define the critical sinter window for achieving full density without compromising dimensional control and mechanical properties are assessed. *In situ* measurements of Contiguity indicate that contiguity decreases at a rate of approximately 0.1/min during the initial minutes after liquid formation, indicating rapid dissolution of tungsten grains in the liquid matrix. The rate of penetration of the neck or grain boundaries is calculated as 0.018 μm/s, and this corroborates with drop in contiguity in the initial few minutes after liquid formation. The reduction in contiguity and connectivity is attributed to the dissolution of the necks between the tungsten grains, from the dissolution rate calculated in this study, it calculated that the grain boundaries dissolve within 3-4 minutes of liquid formation, which is validated by the experiments.

Keywords: Microstructural evolution; Tungsten heavy alloys; Quenching; Contiguity; Sintering temperature

Introduction

Liquid phase sintering is used in net shape fabrication of high performance materials for a wide range of applications [1,2]. Tungsten heavy alloys (WHA) are used in radiation shielding, vibration damping devices, inertial and counter balances, sporting equipment, eccentric weights, penetrators, and other military devices [3]. Prior to liquid formation, WHA undergoes solid-state sintering during heating. Liquid forms at the temperature dictated by the phase diagram of the particular system. Once the liquid forms, the increase in solubility for tungsten induces dissolution of the solid-solid bonds formed during heating [4]. This leads to rapid densification because of the reduction in tungsten tungsten contiguity and skeletal rigidity. If excess liquid forms, continuity and connectivity drop to level where pores are rapidly filled and the concomitant loss of capillarity results in rapid distortion and loss of dimensional control [5-7]. Because of the high alloy density and the large density difference between the solid and liquid, liquid phase sintering of tungsten heavy alloys has a measurable gravitational bias. The density difference between the liquid matrix and the solid grains is about 10 g/cm³ causing pores to rise due to buoyancy and solid grains to settle, resulting in measurable pore and solid gradients. Hence it is critical to manipulate the sintering microstructure to induce densification without distortion [8-10]. In this study we track the process of liquid phase sintering by studying the *in situ* microstructure obtained by quenching a 93W-Ni-Fe (7:3) tungsten heavy alloy. The *in situ* microstructural properties are tracked with temperature and time. Considerable prior work examined microstructure features such as contiguity and grain size versus processing conditions, but after slow cooling so solvated tungsten precipitated to possibly alter the observed micro structure.

Experimental Procedures

The 93% W-Ni-Fe heavy alloys were prepared from elemental W, Ni, and Fe powders. Table 1 summarizes the powder characteristics. The

Powder	Ni	Fe	W (as-received)	W (rod-milled)
Vendor	Novamet	ISP	Osram	
Grade	123	CIP-R1470	M-37	M-37
Purity	99.8%	99.2%	99.5%	99.5%
Type	Carbonyl	Carbonyl	Hydrogen reduction	Hydrogen reduction
Particle Size, μm				
D_{10}	3	2	2	2
D_{50}	10	6	6	3
D_{90}	24	10	10	6
Theoretical density (g/cm³)	8.9	7.9	19.3	19.3

Table 1: Characteristics of W, Ni and Fe powders used in this study.

as-received tungsten powder was de agglomerated by rod milling with pure tungsten rods for 1 h in a 2000 cm³ plastic jar filled with argon. The weight ratio of the rods to the powder was 10:1. Figure 1 show the powders used in this study. The W, Ni, Fe were mixed in 93-4.9-2.1 weight ratio and 0.5 wt% lubricant (Acrawax® C) was added using a Turbula Mixer. The mixed powders were uniaxial die pressed in a Carver Lab Press under at 175 MPa, to form cylinders with a diameter of 12.54 mm and a height of 10 to12 mm. The compacts had a green density of 60% of the theoretical density. The lubricant was removed by heating at 5°C/min at 500°C for 1 h in flowing hydrogen and they presented for

handling strength by heating at 10°C/min to 1000°C for 1 h. Quenching studies were carried out in a vertical quench furnace. The presented sample was suspended in a molybdenum boat and heated at 10°C/min to the desired time-temperature at which time the suspension wire was released, causing the sample to rupture an aluminum membrane to quench into water to freeze the *in situ* microstructure. The quench conditions examined are listed in Table 2.
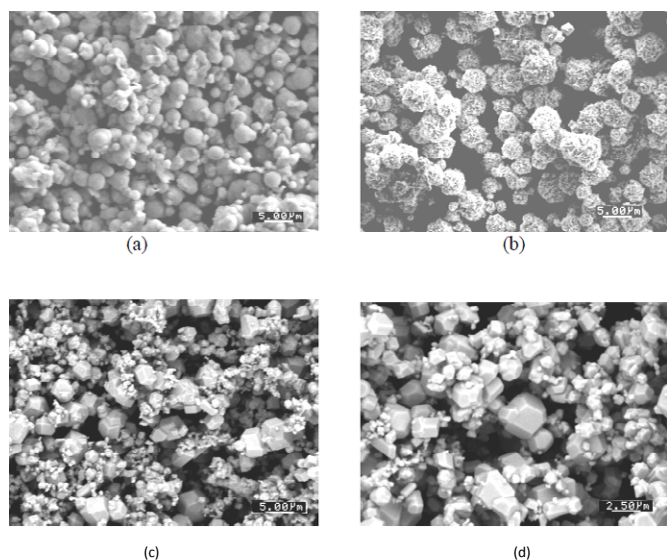

Figure 1: Scanning electron micrographs of (a) Fe (b) Ni (c) W (as-received) (d) rod milled powders.

Quench temperature, °C	Hold time in min at quench temperature
1440	0
1460	0
1475	0
1480	0
1500	0
1500	2
1500	5
1500	10
1500	30

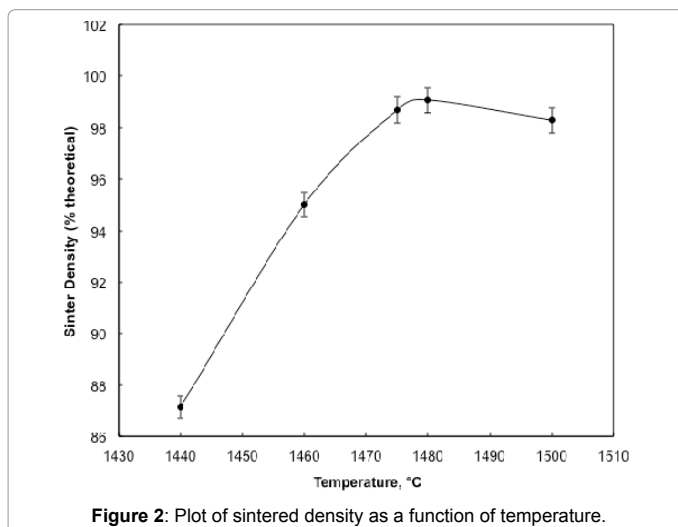**Table 2:** Quench temperature and time combinations.

Figure 2: Plot of sintered density as a function of temperature.
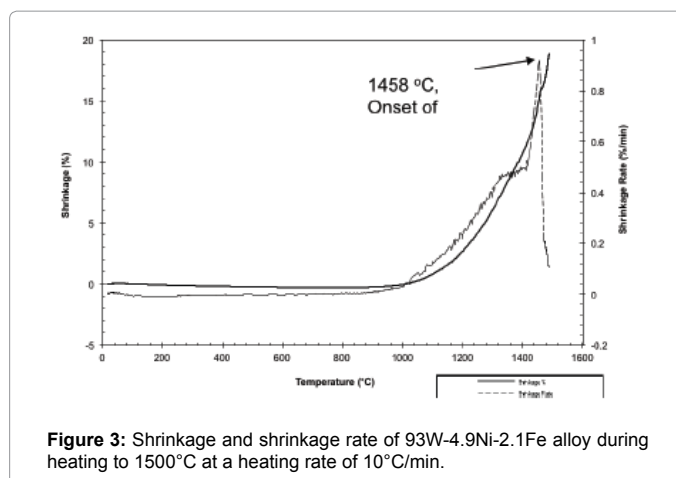

Figure 3: Shrinkage and shrinkage rate of 93W-4.9Ni-2.1Fe alloy during heating to 1500°C at a heating rate of 10°C/min.
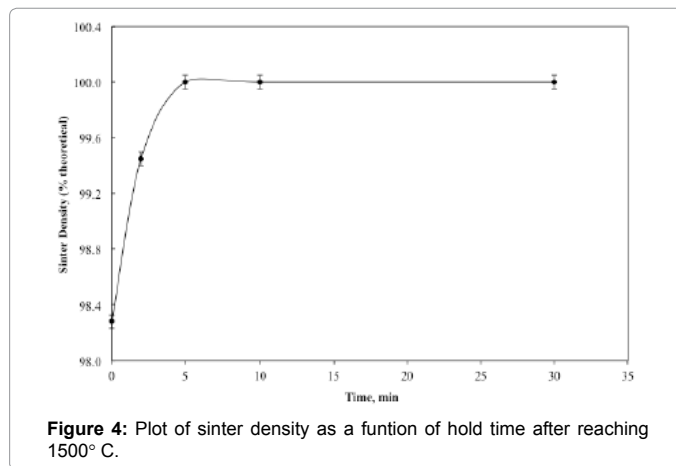

Figure 4: Plot of sinter density as a funtion of hold time after reaching 1500° C.

Results

Sinter density

Figure 2 shows the plot of sinter density of 93 wt% heavy alloy quenched from different temperatures with no hold time. The sinter density increases significantly with temperature and the alloy achieves full density once the liquid is formed above approximately 1458°C. The liquid formation temperature is independently identified by dilatometer as shown in Figure 3. Solid state activated sintering occurs during heating prior to liquid formation, leading to some densification. Once the liquid forms, the liquid provides a capillary force while penetrating the sinter bonds formed during heating, leading to full densification [4]. As seen in Figure 2 the sinter density increases with sinter temperature. The compact is close to full density soon after liquid formation and is fully dense by 1500°C. Figure 4 plots the sinter density change with hold time at 1500°C. Some slight swelling is noted after 5 min, as is often observed for heavy alloys sintered in hydrogen; resulting from oxygen release from the tungsten undergoing solution re precipitation. The released oxygen reacts with hydrogen to form insoluble water vapor. The compact is nearly full dense with no hold at 1500°C but with a few minutes hold the compact achieves full density. Optical micrographs in Figure 5 capture the microstructural evolution. At 1440°C the tungsten grains are bonded into a skeletal structure with irregular pores between the grains (Figure 5a). As temperature increases the pores are eliminated with an increase in density and grain size. The sphericity of the grains also increases.
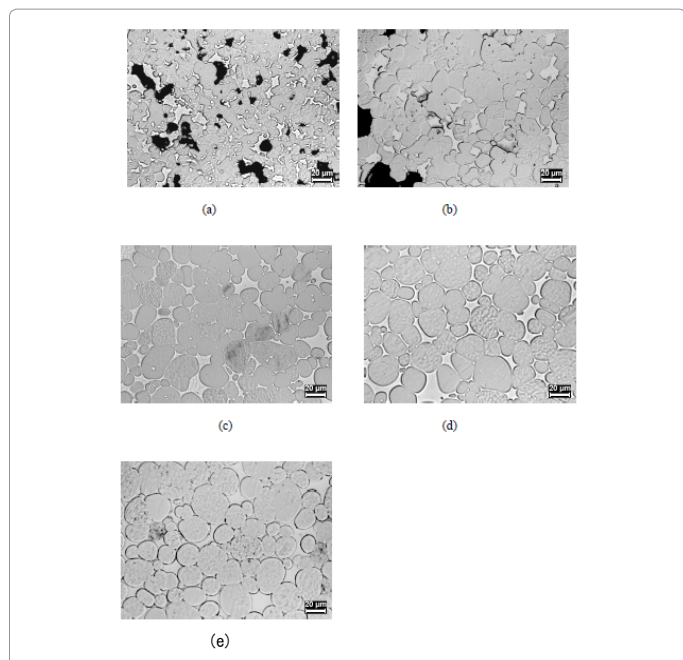
Figure 5: Microstructure of 93W-Ni-Fe (7:3) quenched from different temperatures
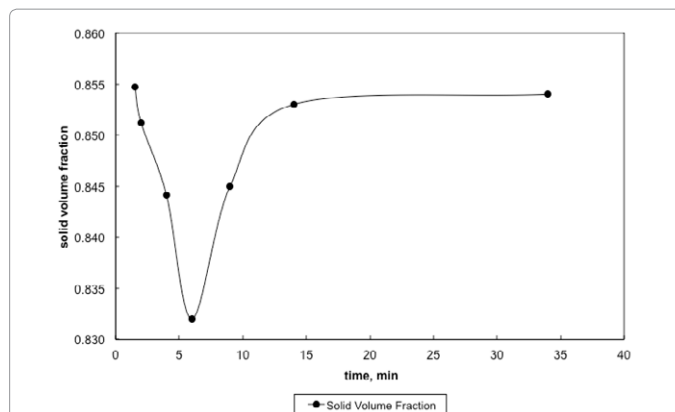a) 1440°C, b) 1460°C, c) 1475°C, d) 1480°C and e) 1500°C.

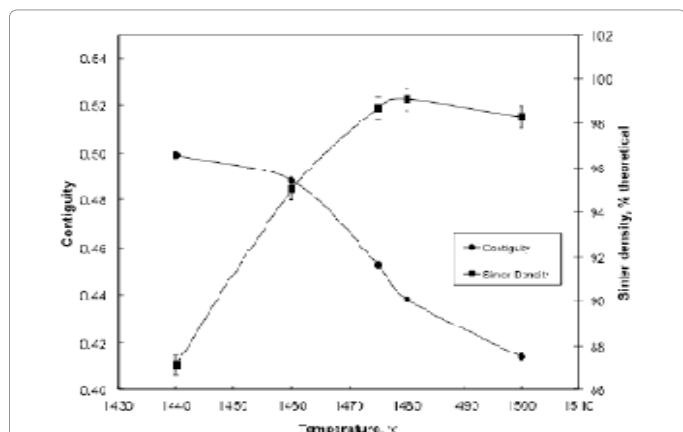**Figure 6:** Plot of continuant sinter density as a function of temperature for a 93W-4.9Ni-2.1Fe alloy during heating to the peak temperature of 1500°C.
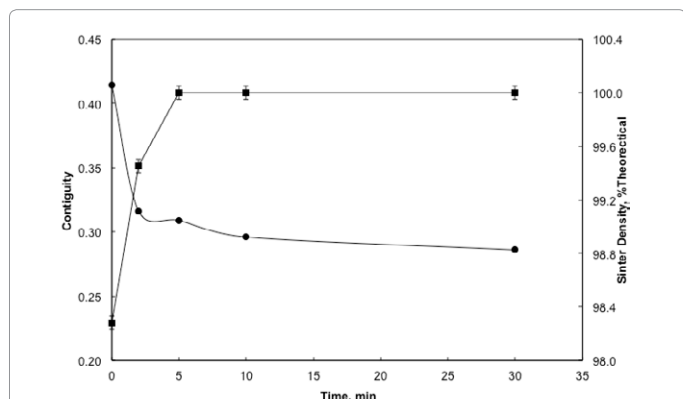

Figure 7: Plot of contiguity and sinter density of 93W-4.9Ni-2.1Fe versus hold time after reaching a peak temperature of 1500°C.

Figure 8: Solid volume fraction as a function of hold time at 1500°C.

Figure 9: Contiguity as a function of time, with 0 corresponding to 1440°C.

Contiguity

The W-W contiguity decreases with an increase in the sintering temperature due to liquid formation and penetration between solid bonds, as shown in Figure 6. The contiguity decrease is steep at 1500°C, where it drops from 0.414 to 0.316 within two minutes of hold. The solid-solid bonds are preferentially dissolved by the newly formed liquid leading to the drop in contiguity (Figure 7). Without the capillary force from pores, such as loss of rigidity results in component slumping. In this experiment the 93W-Ni-Fe (7:3) holds its shape as the amount of liquid is low and densification is delayed and the contiguity remains over a critical value as seen in Figure 8. The slope of the contiguity time plot gives the rate at which contiguity drops and this value is found to be 0.104 /min for the first two minutes hold at1500°C, but then the rate decreases to a value of 0.000526 /min from 2 min to 30 min indicating that the contiguity (dihedral angle) reaches a near constant value, as seen in Figure 9. Contiguity drops at the onset of liquid formation as the liquid formed attacks the solid boundaries. The rate at which this happens is calculated from the slope of the contiguity versus time plot. There exist distinct regions in which contiguity varies differently; contiguity drops steeply in the first few minutes after liquid formation and tungsten solvation, but as saturation is reached in the liquid the system reaches a plateau corresponding to equilibrium saturation and dihedral angle. Upon liquid formation the newly formed melt has more solubility and hence dissolves the grains and the grain boundaries leading to a drop in the solid volume fraction of the 93WNi-Fe alloy, the minimum being attained after 2 minutes at 1500°C. Prior work finds that the heat transfer to supply the melt enthalpy is the slow step, accounting for the timescale for penetration [3]. Connectivity indicates the number of grains an individual grain is in contact with in two dimensions. The mean connectivity was plotted as function of

time at 1500°C. As seen in Figure 10 the connectivity of the alloy drops significantly after a hold time of 30 min. The plot seemingly does not indicate a plateau value at long times.

Discussion

During the heating of tungsten heavy alloy powders sufficient amount of sintering occurs in solid state (nearly 90%) prior to liquid formation [11,12]. Once the liquid forms it lowers the contiguity, weakening the compact and enhancing the densification of the compact [6]. The dissolution is due to the difference in solubility of the tungsten in solid Ni (14.7 at.%) and solubility of tungsten in liquid matrix (20 at.%). The tungsten grains are almost pure tungsten and the matrix has 21 wt.% tungsten in a 90W alloy [13]. Contiguity indicates the strength of the compact and as contiguity decreases the compacts often and densification occurs. The rate of dissolution of the grain boundaries should indicate the rate at which contiguity drops. The contiguity is a ratio of the solid-solid area to the sum of solid-solid and solid-liquid areas. In two dimensions we can assume the linear lengths to represent the areas within the error. So the contiguity for a two sphere model can be given as [2]

$$C_{ss} = \frac{Sss}{S_{SS} + S_{SL}}$$

Using the length of the neck to be SSS and rest of the perimeter of the grain to be SSL we have an equation for contiguity

$$C_{ss} = \frac{X}{4\pi R - X}$$

Taking derivate with time gives

$$\frac{dC_{ss}}{dt} = \frac{4\pi R}{(4\pi R - X)^2} \frac{dX}{dt}$$

We know that the rate of change of contiguity from the slope of the plot as 0.026 at1460°C. Also assuming that the neck size is equal to the radius of the grain (X=R= 4 µm) at 1460°C (from grain size data) the rate of penetration of the neck or the grain boundaries is 0.018 µm/s. This is less than that calculated by Fredriksson et al. [4]. In their experiments the penetration of tungsten grain boundaries by a liquid W-Ni-Fematrix showed that the penetration depth had a parabolic relationship with time. The penetration length "l" depends on time according to the relationship

$$l^2 = \sqrt{\frac{D^L X^L (\Delta \sigma)^2 V_m^L}{8\mu RT (X^{L/s} - X^{S/L})}} \times t$$

The constant term was calculated to be 0.8 ×10-10 m2/s. Dissolution at the solid-liquid interface promotes penetration of grain boundaries with probable velocities in the 0.1 to 2 µm/s range [6]. Our values are
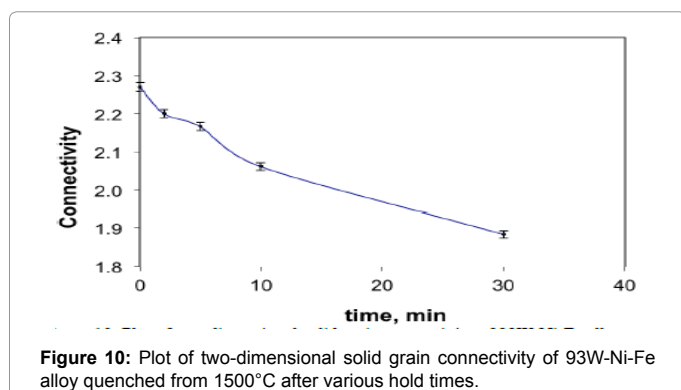

Figure 10: Plot of two-dimensional solid grain connectivity of 93W-Ni-Fe alloy quenched from 1500°C after various hold times.
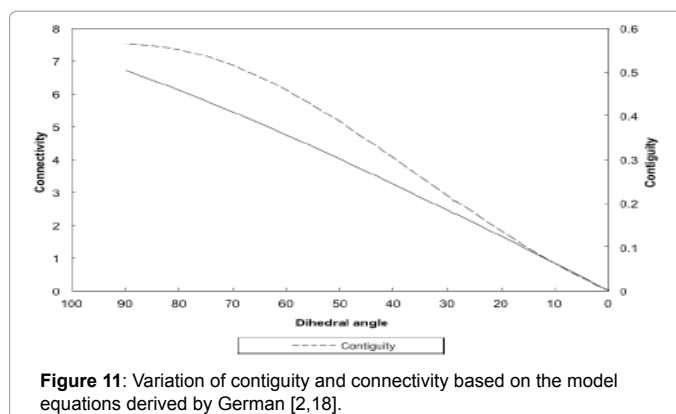

Figure 11: Variation of contiguity and connectivity based on the model equations derived by German [2,18].

an order of magnitude less due to the simplification in the calculation. But this gives a good idea to estimate the rates of dissolution of the grain boundaries. Hence a neck of size of 4 µm should be dissolved in approximately 222 s or3.5 min i.e. the necks dissolve in the first few minutes of the liquid formation. The dissolution of the tungsten grains lowers the solid volume fraction and once the tungsten content in the liquid matrix exceeds equilibrium the tungsten re precipitates on the grain sand the solid volume fraction increases again. Upon liquid formation the solid-liquid surface energy is reduced and hence results in the reduction of dihedral angle [1,6]. Contiguity drops as the dihedral angle decreases. Riegger et al. [14] showed that the contiguity moves through a minimum before it reaches a equilibrium value. They also observed a drastic decrease in dihedral angle in the first few minutes of liquid formation. Contiguity observed in the 93W-Ni-Fe alloy in our study and prior studies [15,16] decreases but doesn't pass through a minimum. This may be due to the fact that more time is required for the equilibrium to be established in this particular system. Chan et al. [17] have shown that the contiguity of the W-8Mo-7Ni-3Fe alloy drops sharply during the initial stage of isothermal holding, and reaches a minimum after an isothermal hold of 120 minutes. The contiguity subsequently increases the grain coalescence mechanism kicks. Microgravity experiments on W-Ni-Cu (6:4) system [18] have indicated that the contiguity decreases for hold time of 180 minutes but increases after a hold time of 600 minutes. More experiments with longer hold times will be needed to verify the increase in contiguity in the 93W-Ni-Fe system. Contiguity depends on the solid volume fraction and the dihedral angle according to the relationship [19]

$$C_{SS} = V_S^2 (0.43 \sin \varphi + 0.35 \sin^2 \varphi)$$

Where, VS is the solid volume fraction which is fixed by fixing the wt.% tungsten in the alloy. Hence as dihedral angle decreases on liquid formation the contiguity decreases. As with contiguity the connectivity also drops as isothermal hold time increases at 1500°C. Connectivity Cg is related to the dihedral angle by the relation [20]

$$C_g = 0.68 N_c \sin(\frac{\varphi}{2})$$

Where NC is the three dimensional co-ordination number and φ is the dihedral angle. As the liquid forms the dihedral angle decreases and as expected from the above equation hence the connectivity decreases. Variation of contiguity and connectivity with dihedral angles based on the above equations is shown in Figure 11. As expected both decrease with a decrease in the dihedral angle. It has been shown that the critical connectivity for shape loss is 3 for various liquid phase sintering systems [8,10]. But these values were calculated at room temperature after cooling. But the connectivity values drop below three for the 93W

alloy and yet there is no shape loss seen in the compact for 93W-Ni-Fe. The average solid volume fraction with a value over 0.85 provides a solid skeleton and the compact retains shape. Hence for evaluating the strength of the compact it is more appropriate to use the *in situ* contiguity and connectivity values as critical values rather than the values obtained at room temperature after cooling.

Conclusions

The sintered density increases with an increase in sintering temperature and time, which is expected. The contiguity decreases with an increase in the sintering temperature and time due to liquid formation. *In situ* measurements of Contiguity indicate that contiguity decreases at a rate of approximately 0.1/min during the initial minutes after liquid

Formation, indicating rapid dissolution of tungsten grains in the liquid matrix. The rate of penetration of the neck or grain boundaries calculated as 0.018 μm/s, and this corroborates with drop in contiguity in the initial few minutes after liquid formation. Maximum reduction in contiguity is observed to occur within a few minutes (3-5 minutes) of the liquid formation. The reduction in contiguity and connectivity is attributed to the dissolution of the necks between the tungsten grains, from the dissolution rate calculated in this study, it calculated that the grain boundaries dissolve within 3-4 minutes of liquid formation, which is validated by our experiments. Further studies are under way to study distortion behavior of heavy alloys. Future experiments involve quenching 88W-Ni-Fe (7:3) and 83W-Ni-Fe (7:3) alloys at different temperatures and correlate their microstructure (contiguity and grain size) to the macroscopic distortion.

Acknowledgement

References

1. German RM (1985) Liquid phase sintering. Plenum Press, New York USA

2. German RM (1996) Sintering theory and practice. John Wiley and Sons, New York USA.

3. Belhadjhamida A, German RM (1991) Tungsten and Tungsten Alloys by Powder Metallurgy –A Status Review," Tungsten and Tungsten Alloys 3-19.

4. Fredricksson H, Eliasson A, Ekbom L (1995) International Journal of Refractory Metal sand Hard Materials 13: 173-179.

5. German RM (1995) Metallurgical and Materials Transactions 26: 279-88.

6. German RM (2001) Manipulation of Strength During Sintering as a Basis for Obtaining Rapid Densification without Distortion. Materials Transactions 42: 1400-1410.

7. German RM (1991) Advances in Powder Metallurgy 4: 183-194.

8. Upadhyaya A, German RM (2000) Materials Chemistry and Physics 67: 25-31.

9. Kipphut CM, Bose A, Farooq S, German RM (1988) Gravity and configurational energy induced microstructural changes in liquid phase sintering. Metallurgical Transactions A 19: 1988-1905.

10. Upadhyaya A, German RM (1988) Metallurgical and Materials Transactions A 2631-2638.

11. Farooq S, Bose A, German RM (1987) Progress in Powder Metallurgy 43: 65-77.

12. Bollina R (2002) Effect of Heating rate on Densification and Distortion in Liquid Phase Sintering of Tungsten Heavy Alloys. M.S Thesis, The Pennsylvania State University, University Park, PA.

13. Bose A, German RM (1988) Metallurgical and Materials Transactions 19: 3100-03.

14. Riegger H, Pask JA, Exner HE (1980) Sintering Processes, edited by Kuczynski GC 219- 233.

15. Chou YH, Zu YS, Lin ST (1996) Materialia 34: 135-40.

16. Bourguignon LL, German RM (1988) The International Journal of Powder Metallurgy 24: 115-121.

17. Chan TY, Lin ST (2000) Microstructural evolution on the sintered properties of W-8 pct Mo-7 pct Ni-3 pct Fe alloy. Journal of Material Science 35: 3759-65.

18. German RM (1985) Metallurgical and Materials Transactions A 16: 1247-1252.

19. Lu P, German RM (2001) multiple grain growth events in liquid phase sintering. Journal of Material Science 36: 3385-94.

20. German RM (1987) Metallurgical and Materials Transactions A 18: 909-914.